Energy dependence of the absorptive potential for sub-Coulomb energy proton bombardment of zirconium and molybdenum isotopes

D. S. Flynn,* R. L. Hershberger, and F. Gabbard
Department of Physics and Astronomy, University of Kentucky, Lexington, Kentucky 40506
(Received 25 June 1984)

The measured (p,p) and (p,n) excitation functions for ^{92,94,96}Zr and ^{95,98,100}Mo were fitted in the energy range $2 < E_p < 7$ MeV using a standard optical model potential with an energy dependent proton absorptive potential. The volume integral of the proton absorptive potential shows strong A dependence at low proton energy and tends to a common value of 100 MeV fm^3 for all isotopes studied as the proton bombarding energy is increased toward 15 MeV. This result is consistent with results from analyses at higher energies.

I. INTRODUCTION

It was first shown by Johnson *et al.*,[1] through study of (p,n) reactions, that the proton absorptive potential is strongly dependent upon A in the mass region near $A=100$, showing a pronounced maximum near $A=103$. In a classic paper[2] on (p,n) reactions on Sn isotopes, Johnson showed that the single particle resonances, specifically the $3p$ resonance in Sn, dominate the behavior of the proton strength function in the energy range from 2 to 7 MeV. In this sub-Coulomb energy region for the bombarding protons, the proton absorption into the compound nucleus is dramatically influenced by the nuclear structure of the target. A qualitative explanation of this effect was described by Lane *et al.*[3] in the context of transition rates to final states in the compound nucleus. The results of Johnson *et al.*[1,2] were confirmed and extended in work at the University of Kentucky through studies of Zr, Mo, Ag, and In nuclei.[4–8] This work confirmed that the volume integral per nucleon of the proton absorptive potential obtained by optical-model analysis of (p,p) and (p,n) cross sections in this mass region exhibits the strong variation with mass number. It was shown[6,7] that the absorptive-potential anomaly persists when the I spin coupling is included in the optical model used to represent the measured cross sections. Calculations with the program ECIS (Ref. 9) show that analysis of the (p,p) and (p,n) cross sections for zirconium and molybdenum isotopes with a deformed potential coupling the ground and first excited (2^+) states of the target yield substantially the same results as analysis with the spherical-optical model. The principal effect of the channel coupling is a reduction of the volume integral of the absorptive potential by 10–20% at each mass number, leaving the anomalous feature changed only slightly. The mass region ($89 \leq A \leq 130$) studied by Johnson[1] begins with a shell closure at 50 neutrons (^{90}Zr) and ends with a proton shell closure at 50 protons (Sn). The nuclear structure progression through the mass region is of undoubted importance in determining the variation of the proton absorptive potential.

Grimes[10] examined two possible explanations of the "anomalous" behavior of W; first, the possibility of collective effects was examined, and second, the expected modulation[1] of the density of intermediate states between shell closures in the mass region was estimated through calculations of 2p-1h states. Grimes concluded, consistent with results presented here, that both effects play a role in explaining the "anomaly." An important result of Grimes's paper[10] is that the "anomaly" in the density of two-particle, one-hole states in nuclei near mass 100 is quite pronounced at 3 MeV, but is markedly reduced at the higher proton bombarding energy of 6 MeV.

Recent measurements of neutron elastic-scattering cross sections of few-MeV neutrons from $Z=39$ to 51 targets by Smith *et al.*[11] showed that the imaginary strength of the optical model potential was strongly shell dependent with pronounced minima at $N=50$ and $Z=50$. Smith concludes that some, but less than the majority, of this effect is attributable to collective-vibrational interactions. Lagrange[12] analyzed neutron scattering measurements from Y, Nb, and Rh and used the resulting optical-model parameters to calculate the proton absorption cross sections which were compared to Johnson's measurements.[1] He suggests that the "anomaly" in part results from neglect of the Coulomb correction to the imaginary terms in the potential. The work of Cereda[13] *et al.* discusses the A dependence in the absorptive strength and concludes that there is no evidence for an anomalous absorptive potential above the Coulomb barrier. Kailas *et al.*,[14] in work on somewhat lighter elements, suggest still other explanations for the variation of absorptive strength with A. Baryshnikov *et al.*[15] have studied elastic proton scattering from ^{109}Ag and conclude that an energy dependent W yields reasonable fits to their data below 6 MeV.

The energy dependence of both the real and imaginary parts of the optical model potential has been extensively treated in the literature for nucleons with energies above about 10 MeV (see, for example, Refs. 16–18 and references therein). However, little information is available about the energy dependence of the imaginary part of the optical model potential below a nucleon bombarding energy of 10 MeV, where nuclear structure effects are expected to play a more important role in the nucleon-nucleus interactions. At low energies where compound nucleus formation is a predominant absorptive process of nu-

 ©1985 The American Physical Society

cleons, the shell structure of nuclei is expected to be an important factor in determining the absorptive strength.[10,11] It is well known that the proton absorptive potential in the standard optical model is independent of energy above about 30 MeV.[17] The volume integral of the empirical potential[17,19,20] averages about 100 MeV fm^3 and is independent of both energy and atomic mass in the energy range from 30 to 60 MeV. It is anticipated, on the basis of these data and these qualitative considerations, that the "anomaly" in the proton-absorptive potential[1] will be most pronounced at low proton bombarding energies where the nuclear structure differences vary most rapidly with A, and that the energy dependence of the absorptive potential should be such that the volume integral for each target tends to the common value of about 100 MeV fm^3 toward the higher bombarding energy. It is to test this hypothesis that the analysis described here was conducted, and it will be seen in what follows that these expectations are substantially verified.

In the work described in the present paper, the energy dependence of the proton-absorptive potential was investigated for the sub-Coulomb energy range $2 \leq E_p \leq 7$ MeV. Six isotopes were studied: ^{92,94,96}Zr and ^{95,98,100}Mo.

II. EXPERIMENTAL METHOD

The measurements were performed using a high voltage Engineering Corporation model CN Van de Graaff accelerator and associated facilities at the University of Kentucky. A beam of protons was used to bombard self-supporting foils of isotopically enriched zirconium and molybdenum to produce (p,p) and (p,n) excitations up to $E_p = 6.7$ MeV. The scattering chamber, the 4π neutron detector, the experimental methods, and uncertainties have been discussed in detail in Refs. 4—6. Table I lists the thickness, the estimated uncertainty in the thickness including foil nonuniformities, and the isotopic enrichment for each target used.

The ^{92,94}Zr(p,p) data were presented in Ref. 6. Those for ^{92,94}Zr(p,n) and ^{95,98}Mo were presented in Ref. 4. The ^{96}Zr, ^{95,98,100}Mo(p,p), and the ^{96}Zr, ^{100}Mo(p,n) excitation functions have been measured to complete the data set. Tables of cross sections for each of the measured reactions are available from the Physics Auxiliary Publication Services.[21]

The energy and angular dependencies of Coulomb scattering have been removed from the (p,p) data by dividing by the calculated Rutherford cross sections. The resulting ratios have been normalized to 1.0 at low energies.

TABLE I. Target data.

Targets	Thickness (μg/cm^2)	Enrichment (%)
^{92}Zr	517±41	95.7
^{94}Zr	914±55	96.1
^{96}Zr	837±13	85.3
^{95}Mo	1073±32	96.8
^{98}Mo	859±60	98.3
^{100}Mo	609±12	92.2

The (p,p) data at 165° are presented in Fig. 1, where the zero of the scale has been suppressed to enhance the deviations from Rutherford scattering. Counting statistics were always less than ±0.5%.

The (p,n) excitation functions are displayed in Fig. 2 as l-averaged experimental strength functions defined by

$$\langle S_{p,n} \rangle \equiv R \frac{\langle \sigma_{p,n} \rangle}{4\pi^2 k^{-2} \sum_l (2l+1) P_l} ,$$

where $\langle S_{p,n} \rangle$ has units of fm, $\langle \sigma_{p,n} \rangle$ is the measured cross section, and P_l is the Coulomb penetration factor for l-wave protons at a radius $R = 1.45A^{1/3}$ fm. The gross features evident in Fig. 2 as a valley at about 3.5 MeV and a broad maximum at about 6 MeV result primarily from the sum of the $3s_{1/2}$ single-particle resonance (SPR) below 2 MeV and the $3p$ SPR at higher energy. These features dominate the strength functions in this mass and energy region.

III. DATA REDUCTION

In order to make it feasible to perform optical model analyses, it was necessary to limit the number of data points used in the analysis. The large number of measured cross sections is apparent in Figs. 1 and 2. The procedure adopted in the present work for the (p,n) cross sections was to select for analysis cross sections at every half MeV.

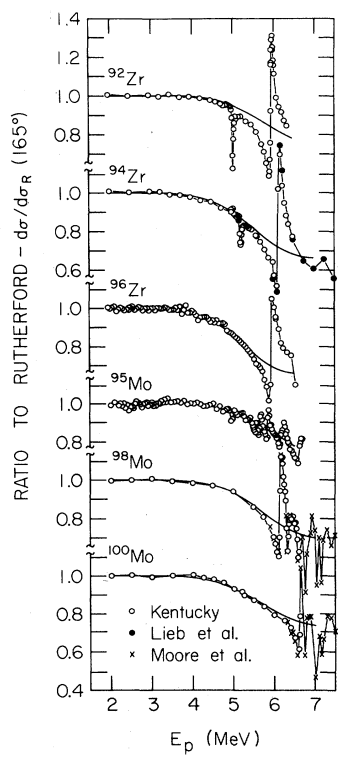

FIG. 1. The (p,p) cross sections at 165° expressed as the ratio to Rutherford for the targets studied, showing the optical model fits described in the text.

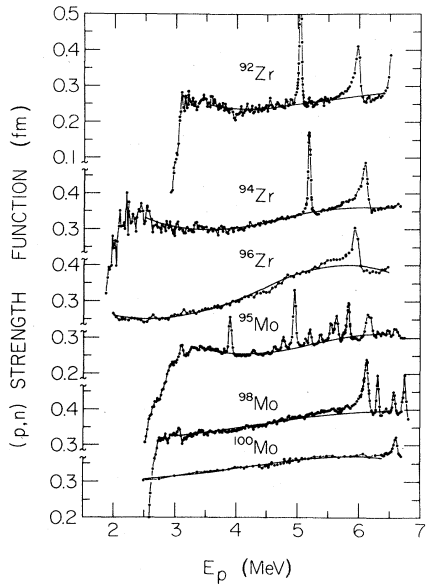

FIG. 2. The (p,n) strength functions for targets ^{92,94,96}Zr and ^{95,98,100}Mo showing the optical model fits described in the text.

These "representative" cross sections were obtained by averaging the measured cross sections lying within $\pm\frac{1}{4}$ MeV of the energy of the representative value. These representative data points are shown as the triangles in Fig. 3.

The open circles in Fig. 3 were obtained by performing Hauser-Feshbach calculations to determine the difference between the total proton-absorption cross sections and the (p,n) cross sections. As illustrated in Fig. 3, the (p,n) and absorption cross sections (or strength functions) are essentially the same, with small differences apparent in ^{92}Zr(p,n) and ^{95}Mo(p,n) at lower energies [near their (p,n) threshold energies]. More details about these calculations can be found in Refs. 1–8. Note that the Hauser-Feshbach calculation of the (p,n) cross section depends on the proton potential and it is the proton potential which will be obtained in an optical-model analysis. For this reason, the Hauser-Feshbach (HF) and optical model calculations were performed iteratively until the results were self-consistent. This procedure was only important for the ^{92}Zr and ^{95}Mo. In these cases the differences between (p,n) and absorption cross sections were so small that the process converged in a couple of iterations.

It is evident in Fig. 2 that isobaric analog resonances (IAR's) are prominent in the cross sections at the higher energies. The (p,p) cross sections were "corrected" to eliminate the effects of the $3s_{1/2}$ IAR which occurs in each of the isotopes studied, and representative (p,p) cross sections were selected which are indicative of the gross structure only. In the selection of representative (p,n) cross sections, the values in the vicinity of the IAR were omitted from the analysis. Previous analyses[6–8] in this mass-energy range have shown that the inclusion of the IAR, in terms of the isospin-coupled Lane model, do not result in significantly different isoscalar potentials.

In order to eliminate the effects of the $3s_{1/2}$ IAR in the (p,p) cross sections, isospin coupled channels calculations were performed in the manner described and with the potential parameters obtained in previous work.[6–8] The calculation of the (p,p) excitation functions at 165° and 135° were then repeated with the isospin coupling set to zero so as to obtain a conventional optical model result. Even though the coupling is set to zero, the isovector part of

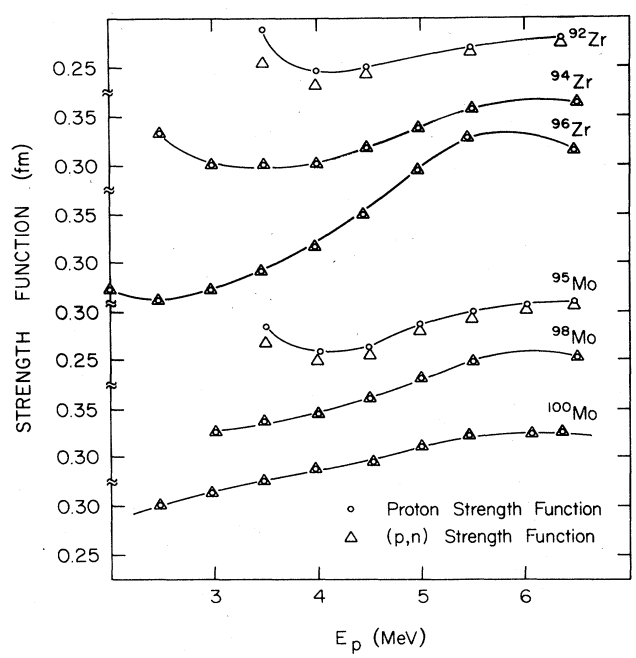

FIG. 3. Proton strength functions (open circles) derived from measurements of the (p,n) strength functions (triangles) corrected for decay channels other than the neutron channels, i.e., (p,p), (p,p′), and (p,γ). The points plotted are the average values for averaging intervals of 0.5 MeV. The points selected avoid isobaric analog resonances.

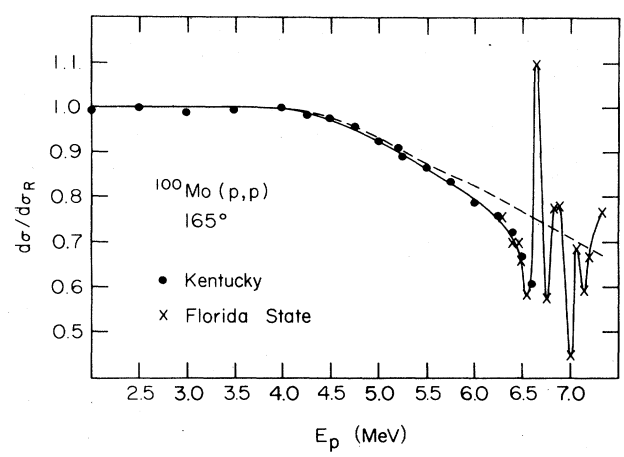

FIG. 4. Differential elastic scattering cross section for ^{100}Mo at a laboratory angle of 165° from measurements of the present work and Ref. 22. The solid line is to guide the eye to the data; the dashed line represents the data after reduction to gross structure of the measured cross sections, i.e., the cross section *without* the contribution of the isobaric analog resonances. See the text.

the real potential is left intact to yield the conventional asymmetry terms.

The differences between the results obtained with and without coupling (with and without the occurrence of the $3s_{1/2}$ IAR in the resulting cross sections) were then used to correct the measured cross sections and obtain cross sections representative of the gross structure. These differences were scaled from nucleus to nucleus to account for the fact that the calculations assume unit spectroscopic factors.

The results of the procedure are illustrated for ^{100}Mg(p,p) in Fig. 4. Also illustrated is the fact that other measurements (crosses in Fig. 4 are from Moore *et al.*[22]) were used to determine the representative data points at higher energies. These higher energy points were qualitatively selected by drawing a smooth curve through the data.

IV. OPTICAL MODEL ANALYSIS

The analysis of the (p,p) and the (p,n) data, as described in Sec. III, was performed using a standard optical model (SOM) potential whose form is given in Refs. 5 and 6. As is customary, a volume Woods-Saxon potential was used for the real form factor and a surface (derivative) Woods-Saxon was taken for the imaginary part of the potential. The strength of the real potential is defined as follows:

$$V_R(E)=V_R(0)-0.32E \ ,$$

$$V_R(0)=V_0+24(N-Z)/A+0.45Z/A^{1/3} \ .$$

In previous analyses,[4–8] the effects of various modifications to the SOM upon the values of the parameters and upon the goodness of fit to the data sets have been tested. It has been shown that the proton-absorptive-potential anomaly persists when I spin coupling[6,7] and nuclear deformation are introduced into the potential. The SOM potential used in the present analyses differs from that in Refs. 5 and 6 in that the strength of the imaginary part of the potential was taken to be

$$W_D=W_0+(dW_D/dE)E$$

in the proton bombarding energy range from 2 to 7 MeV. As discussed earlier, the energy dependence is anticipated on physical grounds. A linear form was assumed for simplicity. The fixed parameters of the SOM analysis were as follows: $V_{so}=6.4$ MeV, $r_{so}=1.03$ fm, $a_{so}=0.63$ fm, $r_R=1.2$ fm, and $r_D=1.3$ fm; the Coulomb radii were determined as described in Ref. 5.

The optical-model analyses were performed with the computer code GENOA.[23] This code automatically adjusts specified optical-model parameters to minimize the difference between data points and computed values as expressed by χ^2, which is defined by

$$\chi^2=\frac{1}{N}\sum_{i=1}^{N}\left[\frac{\sigma_i^{\text{exp}}-\sigma_i^{\text{th}}}{\Delta\sigma^{\text{exp}}}\right]^2 ,$$

where N is the number of values of the cross sections in the data sets being fitted. The data points used in the fitting procedure were derived from the (p,n) and (p,p) measurements as described in Sec. III. The σ_i are the experimental and theoretical cross sections and $\Delta\sigma_i^{\text{exp}}$ is the estimated error in the measured cross section values. For the purposes of the analysis, the error at each data point was taken to be the average value of 1%, except that an error of 2% was used as the estimate in the higher energy region where (IAR's) increase uncertainties in the average cross sections.

As described in Sec. III, the (p,p) and the HF corrected (p,n) cross sections were fitted in a sequence of two, three, and four parameter searches. The best values of the parameters of each search and the corresponding minimum value of χ^2 for each target nucleus are given in Table II. The results of the two, three, and four parameter fits to ^{92}Zr are shown in Fig. 5.

The guiding principle of the search procedure was that as many SOM parameters as possible should be fixed at their "global" values consistent with the requirement that good fits to the data be obtained. The position and spreading width of the SPR in each isotope studied is determined primarily by the values of V_R and W_D, respectively.[1,2,4] The value of the imaginary diffuseness parameter, a_D, also affects the shape of the SPR; however, the effect is more nearly a normalization shift in the fit, whereas W_D affects the width. Fitting both the absolute magnitude and the shape of the strength functions effectively removes the well-known W_Da_D ambiguity.[24] The requirement that the (p,p) data at 135° and 165° be fitted provides added constraints on the parameters, as has been shown by Schrils *et al.*[6] Starting values of a_D, the imaginary diffuseness, given in Table II were fixed as obtained from previous analyses.[4,7] Values of other fixed parameters have already been given.

The two-parameter search gave poor fits except for ^{100}Mo and grew progressively worse toward the smaller values of A (^{92}Zr). This indicated that model variations more complex than simply readjusting V and W were required. Schrils *et al.*[6] had found that the real diffuseness a_R needed to be adjusted to fit the (p,p) data. A three-parameter search on V_0, W_D, and a_R was then carried out. The resulting fits illustrated for ^{92}Zr in Fig. 5 are better than the two-parameter fits for the (p,p) data, but the strength function (SF) is fitted poorly.

To further improve the fit to the data, a fourth parameter was chosen for variation. The choice of this fourth parameter was made after study of the sensitivity of χ^2 to the variation of the various potential parameters of the model. Results for five different candidates for the fourth parameter are illustrated in Fig. 6. This shows that the fit for ^{92}Zr is highly sensitive to the value of dW_D/dE, the energy dependence of the imaginary potential. This observation plus the expectation on physical grounds that W_D should be sensitive to nuclear structure at low bombarding energies led to the choice of dW_D/dE as the fourth parameter to be varied.

It is seen in Fig. 5 that the four-parameter fit to ^{92}Zr is excellent. Values of dW_D/dE for the six nuclei are given in Table II. Similar quality of fits were obtained for all nuclei studied, as is shown by the values of χ^2 determined for the four-parameter search. The excitation functions calculated from these fits are shown as solid curves in Figs. 1 and 2 for comparison with the experimental data.

TABLE II. Parameters obtained in optical model (OM) fits to data. Note that: (a) The assumed error for χ^2 is 1%. (b) For the four-parameter search, the imaginary part of the potential is varied with energy (2 MeV $< E_p <$ 7 MeV) according to the relation $W_D = W_0 + (dW_D/dE)E_p$. (c) All a_D are adopted from previous analyses (Refs. 4 and 7). They are within 10% of 0.4 fm. (d) a_R was set equal to 0.73 fm in the two-parameter search.

		Two parameter search			Three parameter search				Four parameter search			
Isotopes	a_D (fm)	V_0 (MeV)	W_D (MeV)	χ^2	V_0 (MeV)	W_D (MeV)	a_R (fm)	χ^2	V_0 (MeV)	W_0 (MeV)	a_R (fm)	dW_D/dE	χ^2
^{92}Zr	0.40	53.6	5.6	31	53.5	9.1	0.65	6.7	53.1	−5.76	0.64	3.09	1.2
^{94}Zr	0.42	53.3	9.9	8.5	53.4	11.2	0.72	5.1	53.2	+2.08	0.72	1.83	1.5
^{96}Zr	0.37	55.0	10.8	4.2	55.3	11.2	0.72	2.7	54.1	3.67	0.75	1.63	1.6
^{95}Mo	0.40	53.9	7.4	13.3	54.2	11.1	0.68	3.4	53.4	−6.59	0.68	3.47	1.4
^{98}Mo	0.44	54.8	13.8	2.8	53.6	13.8	0.74	1.8	56.5	28.4	0.71	−2.74	1.4
^{100}Mo	0.42	53.4	16.4	1.3	53.0	16.7	0.73	1.2	54.2	23.3	0.72	−1.28	1.0

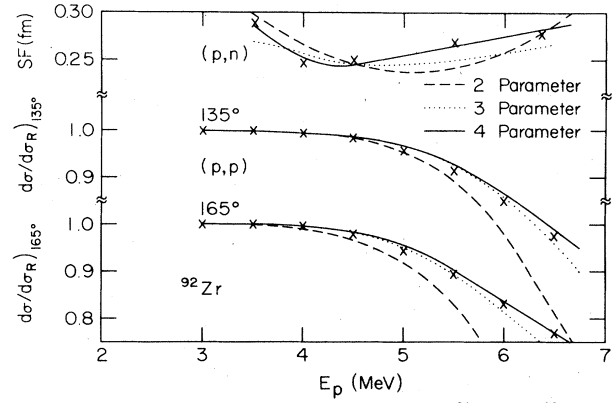

FIG. 5. Representative data points for ^{92}Zr(p,p)^{92}Zr and ^{92}Zr(p,n)^{92}Nb compared with optical model calculations. The points represent averaged data as illustrated in Fig. 3. The dashed, dotted, and solid lines represent two, three, and four parameter OM fits to the data as described in the text.

V. DISCUSSION OF THE ABSORPTIVE POTENTIAL

The analysis discussed in the preceding section resulted in absorptive potentials which were linearly dependent on the proton energy. The slopes (dW_D/dE) and intercepts (W_0) vary drastically, significantly differing from values obtained in other analyses of both proton[16,24,25] and neutron potentials.[17,24,26] Throughout the range of measured

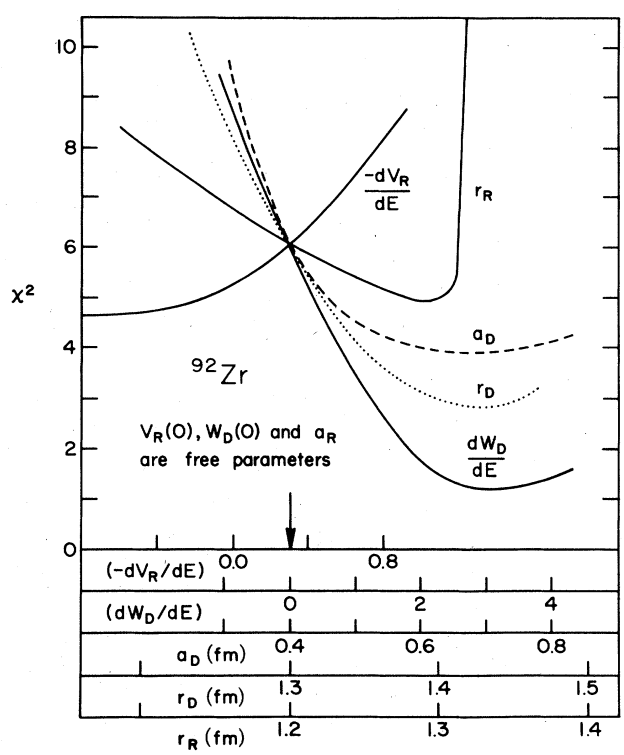

FIG. 6. Sensitivity of χ^2 to the variation of selected parameters for ^{92}Zr. For each value of the parameter indicated, V_0, W_0, and a_R were varied to obtain the minimum χ^2. The arrow indicates the fixed values used for the three parameter search.

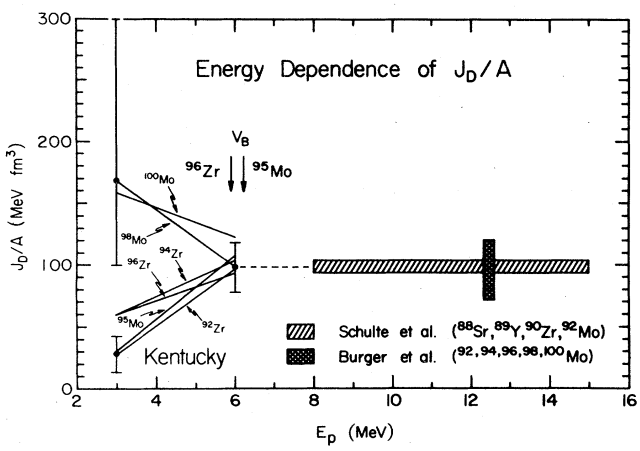

FIG. 7. Energy dependence of the volume integral per nucleon of the absorptive potential, W, resulting from the four parameter search. Solid lines below 6 MeV show the rapid energy dependence in the absorptive potential derived from optical model fits to the (p,n) and (p,p) data. Error bars indicate a range of values of W resulting from acceptable fits. The arrows labeled V_B indicate the Coulomb barrier height for ^{96}Zr and ^{95}Mo. The high energy results are from the measurements of Refs. 19 and 20.

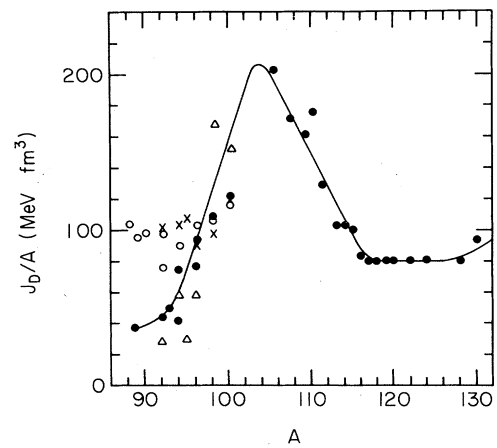

FIG. 8. Volume integral per nucleon of the absorptive potential for mass-100 nuclides. Solid circles represent the results of previous optical model analyses of (p,n) cross sections (Refs. 1, 4, 5, and 7). Open circles represent the results of optical-model analyses (Refs. 19 and 20) of proton scattering measurements for proton energies which are above the Coulomb barrier (8—15 MeV). Crosses represent the present energy dependent result at a proton energy of 6 MeV. Triangles represent the present result at a proton energy of 3 MeV and illustrate the increasing importance of the nuclear structure at low energy.

proton energies, the absorptive potentials vary as shown in Fig. 7. Also shown in Fig. 7 are the results of optical model analyses of proton scattering excitation functions measured by Schulte *et al.*[20] and proton scattering angular distributions measured by Burger *et al.*[19] To facilitate comparisons between the different potentials, the volume integrals per nucleon are plotted. The energy range measured by Schulte *et al.* is indicated in the figure. The results of Burger *et al.* for Mo isotopes were obtained at 12.5 MeV.

A striking aspect of the present result is that at the higher energies (6—7 MeV), the absorptive potential strengths converge to values around 100 MeV fm^3, values comparable to the results of Burger *et al.* and Schulte *et al.* The error bars shown on the present results illustrate the maximum ranges through which the absorptive potentials varied in the course of calculations, for reasonable changes in the data and the fixed parameters. Throughout various calculations, the largest differences occurred in the absorptive potentials of the larger two masses at the lower energies. This is related to the fact that the larger masses have highly damped single-particle resonances (larger absorptive potentials) at the low energies, and hence, less sensitivity to variation of the absorptive potential, W_D.

The consistency of the present results is illustrated in Fig. 8, where the volume integrals of the absorptive potentials are plotted versus mass number. Previous results of optical model analyses of (p,n) data alone are represented by the solid circles. The results of Schulte *et al.*[20] and Burger *et al.*[19] are represented by the open circles. The present energy dependent absorptive potential is shown as the crosses for 6 MeV proton energy and as the triangles for 3 MeV proton energy. Again it is evident that, at the higher energies, the present result is consistent with the results of analyses of measurements made at energies above the barrier, whereas the results at the lower energies show nuclear structure effects first observed by Johnson *et al.*[1] The finding of an energy dependent W_D is also consistent with the two-particle, one-hole level density calculation of Grimes[10] showing the diminution of the structure effect on W as the bombarding energy is increased. The cumulative evidence concerning the "anomaly" in the imaginary part of the optical potential strongly supports the hypothesis that it is a manifestation of the shell structure of the nuclei in this mass range.

ACKNOWLEDGMENTS

The help of York Dobyns, Sally Fisher, Ben Luntz, and Michael Smith, who assisted in the data taking and the data analysis, is gratefully acknowledged. The authors are most grateful to Cleland Johnson of the Oak Ridge National Laboratory and to Stephen M. Grimes of Ohio University for helpful discussions. This work was supported by the National Science Foundation under Grant No. PHY 8105672.

*Present address: Nichols Research Corporation, 4040 South Memorial Parkway, Huntsville, AL 35805.

[1]C. H. Johnson, A. Galonsky, and R. L. Kernell, Phys. Rev. Lett. **39**, 1604 (1977); Phys. Rev. C **20**, 2052 (1979).

[2]C. H. Johnson, J. K. Bair, C. M. Jones, S. K. Penny, and D. W. Smith, Phys. Rev. C **15**, 196 (1977).

[3]A. M. Lane, J. E. Lynn, E. Melkonian, and E. R. Rae, Phys. Rev. Lett. **2**, 424 (1959); J. E. Lynn, *Theory of Neutron Resonance Reactions* (Clarendon, Oxford, 1968), Chap. 6, p. 280ff.

[4]D. S. Flynn, R. L. Hershberger, and F. Gabbard, Phys. Rev. C **20**, 1700 (1979).

[5]R. L. Hershberger, D. S. Flynn, F. Gabbard, and C. H. Johnson, Phys. Rev. C **21**, 896 (1980).

[6]R. Schrils, D. S. Flynn, R. L. Hershberger, and F. Gabbard, Phys. Rev. C **20**, 1706 (1979).

[7]D. S. Flynn, R. L. Hershberger, and F. Gabbard, Phys. Rev. C **26**, 1744 (1982).

[8]D. S. Flynn, Phys. Rev. C **27**, 2381 (1983).

[9]J. Raynal, Saclay Report No. IAEA-SMR-918, 1972; J. Raynal, in *Computing as a Language of Physics* (IAEA, Vienna, 1972); M. A. Melkanoff, J. Raynal, and T Sawada, Math. Comput. Phys. **6**, 2 (1966).

[10]S. M. Grimes, Phys. Rev. C **22**, 436 (1980).

[11]A. B. Smith, P. T. Guenther, and J. F. Whalen, Nucl. Phys. **A415**, 1 (1984).

[12]Ch. Lagrange, Phys. Rev. C **22**, 896 (1980).

[13]E. Cereda, M. Pignanelli, S. Micheletti, H. V. von Geramb, M. N. Harakeh, R. De Leo, G. D'Erasmo, and A. Pantaleo, Phys. Rev. C **26**, 1941 (1982).

[14]S. Kailas, M. K. Mehta, S. Gupta, Y. P. Viyogi, and N. K. Ganguly, Phys. Rev. C **20**, 1272 (1979).

[15]A. I. Baryshnikov, A. F. Gurbich, and N. N. Titarenko, Yad. Fiz. **37**, 529 (1983) [Sov. J. Nucl. Phys. **37**, 315 (1983)].

[16]D. M. Patterson, R. R. Doering, and Aaron Galonsky, Nucl. Phys. **A263**, 261 (1976).

[17]J. Rapaport, Phys. Rep. **87**, 27 (1982).

[18]J.-P. Jeukenne, A. Lejeune, and C. Mahaux, Phys. Rev. C **16**, 80 (1977); **15**, 10 (1977).

[19]S. J. Burger and G. Heymann, Nucl. Phys. **A243**, 461 (1975).

[20]K. Schulte, G. Berg, P. von Brentano, and H. Paetz gen. Schieck, Nucl. Phys. **A241**, 272 (1975).

[21]See AIP document No. PAPS PRVCA 20-1700-6 for ^{92,94}Zr and ^{95,98}Mo(p,n) cross sections. See AIP document No. PAPS PRVCA 26-1744-5 for ^{96}Zr, ^{100}Mo(p,n) cross sections. See AIP PAPS PRVCA 31-87-11 for ^{92,94,96}Zr and ^{95,98,100}Mo(p,p) cross sections. Order by PAPS number and journal reference from American Institute of Physics, Physics Auxiliary Publications Service, 335 East 45th Street, New York, NY 10017. This material also appears in Current Physics Microfilm, the monthly microfilm edition of the complete set of journals published by AIP, on frames immediately following Ref. 4, Ref. 7, and this journal article, respectively.

[22]C. F. Moore, P. Richard, C. E. Watson, D. Robson, and J. D. Fox, Phys. Rev. **141**, 1166 (1966); K. P. Lieb, J. J. Kent, T. Hausmann, and C. E. Watson, Phys. Lett. **32B**, 273 (1970).

[23]F. G. Perey (private communication).

[24]C. M. Perey and F. G. Perey, At. Data Nucl. Data Tables **17**, 1 (1976).

[25]F. D. Becchetti, Jr. and G. W. Greenlees, Phys. Rev. **182**, 1190 (1969).

[26]J. Rapaport, V. Kulharni, and R. W. Finlay, Nucl. Phys. **A330**, 15 (1979).